Polish J. of Environ. Stud. Vol. 19, No. 2 (2010), 301-308

Original Research

Synthesis of Modified Mesoporous Materials and Comparative Studies of Removal of Heavy Metal from Aqueous Solutions

Ping Ge, Fengting Li*, Bingru Zhang

State Key Lab of Pollution Control and Resource Reuse Study,
College of Environmental Science and Engineering,
Tongji University, 200092 Shanghai, China

Received: 1 June 2009
Accepted: 16 August 2009

Abstract

The functionalized mesoporous' potential ability of binding heavy metals using different templates, namely cetyltrimethylammonium (CTAB) (adsorbent A) and triblock copolymer (Pluronic P123, EO20PO70EO20, Mav = 5800) (adsorbent B), was evaluated. The synthesized materials were characterized by powder X-ray diffraction (XRD), nitrogen gas sorption, FT-IR and solid-state ^{13}C and ^{29}Si NMR spectroscopy and thermogravimetry (TGA) measurements. In the adsorption experiment, the effects of several variables (stirring time, pH and presence of other metals in the medium) were studied. On the basis of these results, it was observed that the adsorption capacities were higher for adsorbent B than adsorbent A. The results also confirmed that the ureido group ($CO\text{-}NH_2$) has a good affect of binding metal ion.

Keywords: mesoporous silica, modified, character, heavy metal, removal

Introduction

With the development of industrial production, large quantities of heavy metals have been released into the natural environment. Heavy metals are mostly toxic, even at very low concentrations. For example, copper is a trace element essential to life, the total copper of the normal human body is about 100-150 mg. Excessive intake of copper is toxic to humans. The harmful effects include a number of disorders, such as making active protein in the body invalid, causing itching, and skin inflammation. In order to remove heavy metal from aqueous solutions, an encouraging branch of techniques have evolved in recent years involving the synthesis of designed materials [1-4].

Many chemical and biological treatments have been applied in the removal of heavy metal from waters [5-11]. Mesoporous materials functionalized with various organic groups are among the most popular methods used to control such pollutants [12-15].

The preparation of mesostructured silicas since 1992 [16] has opened a wide field of applications [17-19]. Main research interests have focused on the use of non-ionic surfactants or ionic liquids for synthesis [20, 21], the characterization of materials by advanced techniques [22, 23], and potential applications of new materials in adsorption or catalysis [24-26]. Functionalization of these materials has gained recognition as the most exceptional adsorbents for heavy metal [27-32]. The incorporation of functionalities can be achieved by:

(a) "Two-step" procedure: grafting the organic component onto a pure silica matrix (namely post-synthesis treatment),
(b) "One-step" procedure: co-condensation of inorganic silica species with a silylating organic compound, and

*e-mail: fengting@tongji.edu.cn

(c) using bisilylating organic precursors that lead to mesoporous organo silicas.

The three methods have different advantages and disadvantages. Post-synthesis has the advantage of easily leading to the morphology destruction and the disadvantage of a low ratio of modified functional groups. Meanwhile, co-condensation, as we know, has a uniform distribution of functional groups inside the mesopore channels with a shortage of smaller pore size [33-34]. Using bisilylating organic precursors is rarely reported.

The mesoporous materials bearing such groups as thiol [35-37] and amino [38-40] often have been reported. However, reports about ureido-modified mesoporous materials are scarce. Moreover, few reports have compared the ability of different templates the synthesize mesoporous binding ureido as adsorbents.

In this paper, rarely used A-1160 ($(C_2H_5O)_3SiC_3H_6NHCONH_2$, Mav=222.4, bearing ureido) as a binding group modified by mesoporous adsorbents were fabricated and the adsorption character of different adsorbents binding ureido using various structure-directing agents (P123 and CTAB) were compared [41].

Experimental Procedures

Synthesis of Adsorbent A

The synthesis of adsorbent A was carried out according to [34] using cetyltrimethylammonium (CTAB) and tetramethylammonium hydroxide (TMAOH) as hybrid surfactant templates, and tetraethyl orthosilicate (TEOS, 98%, MAV=208.33) as the silica source. The typical synthesis process is as follows: 2.19 g CTAB was dissolved in 40 g dry ethanol at room temperature and stirred for 2 h. In the meantime, 2.22 g A-1160, 3.6 g TMAOH and 20 g dry ethanol were mixed and also stirred for 2 h. Then 6.6 g TEOS was slowly added into the mixed solution of the above two to obtain a gel (the molar composition of the mixture was 0.25 A-1160: 1TEOS: 0.188 CTAB: 0.309 TMAOH: 40.76 ethanol). After 1 h stirring, the result was transferred into a Petri dish for solvent evaporation. The product slurry was transferred inside a polypropylene bottle at 90ºC for 3 d under static conditions. After filtration, it was then submitted to a continuous reflux run overnight in ethanol/HCl at 70ºC to extract the surfactant templates. Then it was filtered, stirred with 1 mol/L $NaHCO_3$ solution for 24h and washed with deionized water for neutralization. Finally, it was dried under vacuum.

Preparation of Adsorbent B

Preparation of adsorbent using a triblock copolymer (Pluronic P123, EO20PO70EO20, Mav = 5800) was similar to that used in synthesis of adsorbent A with CTAB, except that 4 g P123 replaced 2.19 g CTAB, 0.4 g HCl and 3.6 g H_2O replaced 3.6 g TMAOH.

Metal Ion Adsorption on the Functionalized Mesoporous Silica

Metal nitrates (analytical grade) were dissolved in deionized water in order to prepare the initial metal ion solution with different concentrations (1, 2, 10 mmol/l, respectively). In a typical run, approximately 50 mg of each mesoporous silica A, B, and 10 ml metal ion solution were placed in stoppered vials and subject to ultrasound for 25 min. at room temperature.

Effect of the pH

Metal nitrates (analytical grade) were dissolved in deionized water with a concentration of 1 mmol/l. The solution was adjusted to desired pH levels ranging from 2 to 7. 10 ml of above solutions and approximately 50 mg adsorbent B were placed in stoppered vials and subject to ultrasound for 25 min. at room temperature. The resulting solution was separated by a 0.45 μm Uniflo filter and the filtrate was analyzed using ICP/OES spectroscopy.

Metal Ion Competitive Adsorption

Ion competitive adsorption studies were performed by treating 10 mL of a mixed metal solution containing equimolar amounts (1 mmol/ L of Cu^{2+} + Co^{2+}, Cu^{2+} +Ni^{2+} and Cu^{2+} + Zn^{2+} ions) with 50 mg of adsorbent B for 25 min. sonicating, at room temperature. The resulting solution was separated by a 0.45 μm Uniflo filter and the filtrate was analyzed using ICP/OES spectroscopy.

Results and Discussion

Solid-State NMR Spectra

The successful grafting of the functional groups on mesoporous MCM-41 can be proven by the solid-state NMR spectra.

Fig. 1 depicts the ^{13}C CP-MAS NMR spectra of MCM-41 with ureido using CTAB and P123 as directing agent, respectively ((a) and (b)). The ^{13}C CP-MAS NMR spectrum of ureido-grafted MCM-41 using CTAB as agent shows 7 peaks at chemical shifts at 9 ppm, 15 ppm, 23 ppm, 33 ppm, 43 ppm, 57 ppm, and 161 ppm. The three carbon atoms related to the ligand ring, numbered 3, 4, and 5, give signals at 9 ppm, 15 ppm, and 33 ppm, respectively. The signal due to methylene 2 of the ethoxy group appears at 57 ppm and the signal of the methyl group at 23 ppm. The aromatic carbon labeled 6 is assigned to the signal at 161 ppm. Finally, the signal due to the methyl in the heterocycle numbered 7 appears at 43 ppm. These results provide evidence that the preparation of the new material was successful.

The solid-state ^{29}Si MAS-NMR spectra for both ((a) and (b)) confirm the covalent bond formed between the silylating and the silanol groups dispersed on the MCM-41 surface (Fig. 2). Unmodified groups show two main peaks

at -110 and 102 ppm, and these are assigned to Q4 and Q3 silanol sites, respectively [27,44]. Both of the figures show Q4 and Q3. In addition, two new peaks appear at -55 and -62 ppm, which are assigned to T2 ($(SiO)_2SiOH$-R) and T3 ($(SiO)_3Si$-R sites, respectively.

FT-IR

The adsorbents were characterized by FTIR to ascertain the modification of ureido. The FTIR patterns present locations and appearances similar to the major bands in Fig. 3. The features around 1,074 cm^{-1} and 959 cm^{-1} indicate Si-O-Si and Si-O-H stretching vibrations, respectively. The bands around 789 cm^{-1} and 457 cm^{-1} result from Si-O-Si vibrations. The spectra of samples show characteristic bands for methane-stretching vibrations around 3,000-2,800 cm^{-1}. There is also strong evidence for successful grafting of functional groups [42].

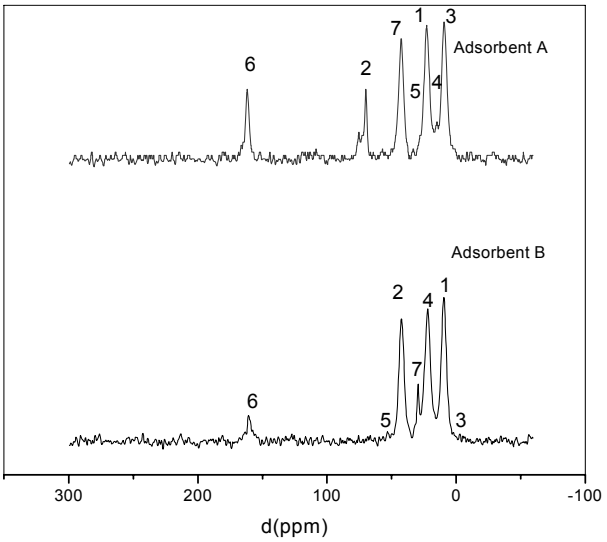

Fig. 1. Solid-state ^{13}C CP-MAS NMR spectra of adsorbent (A) and adsorbent (B).

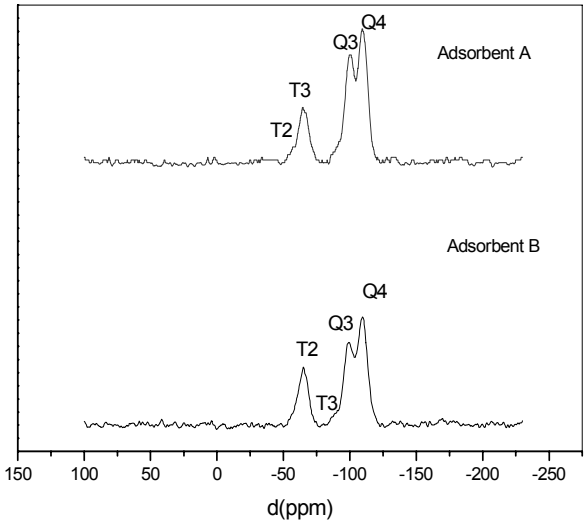

Fig. 2. Solid-state ^{29}Si MAS-NMR of adsorbent (A) and adsorbent (B).

Thermogravimetry

An important aspect of the prepared materials is their thermal stability. Thermogravimetric analyses of mesoporous materials were performed under nitrogen atmosphere

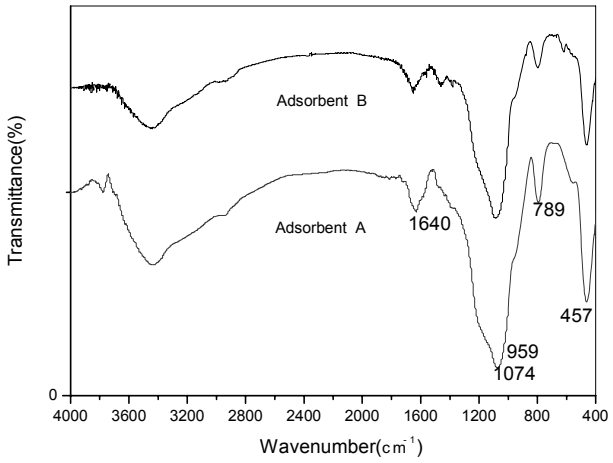

Fig. 3. FTIR spectra of adsorbent A and B.

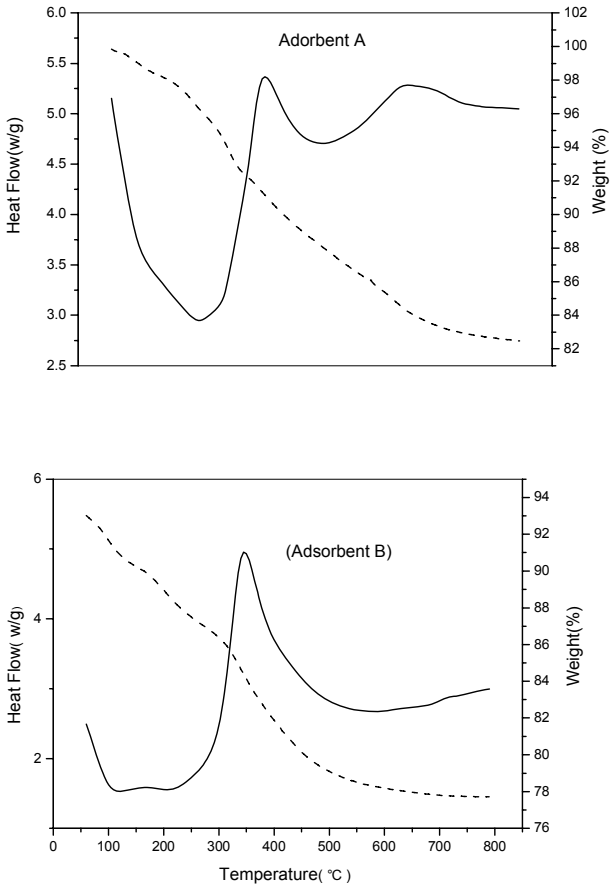

Fig. 4. Thermogravimetric analysis of adsorbent (A) and adsorbent (B).

Table 1. Physical parameters of mesoporous material (adsorbent A and adsorbent B) measured by N_2 adsorption-desorption isotherms.

Sample	BET surface area (m^2/g)	Total pore volume (cm^3/g)	Pore diameter (BJH) (nm)
Adsorbent A	546.1	0.79	4.29
Adsorbent B	347	0.68	7.90

from room temperature to 800ºC at a rate of 10ºC/min to test the thermal stability of the samples (Fig. 4). The weight of the samples was studied as a function of temperature. The profiles indicate that both of the samples show a small loss in mass (4.3%) between room temperature and 100ºC due to the loss of physically adsorbed water (endothermic process). A second decrease in mass of 0.6% (between 600 and 800ºC) is attributed to the increase in the number of siloxane bridges (Si-O-Si) due to isolated silanol condensation (exothermic process). The TGA curves of the modified material (A and B) show that a degradation process occurs between 310 and 500ºC and that weight loss is about 15%. This is due to the breakdown of pendant groups anchored on the silica surface (exothermic process). The thermal stability of these samples is in agreement with previous results given in the literature [43].

X-Ray Diffraction (XRD) Tests

The XRD patterns for mesoporous silica are shown in Fig. 5. The decrease of the (100) XRD diffraction peak showed that the attachment of organic functional groups in the mesopore channels tends to reduce the scattering power of the mesoporous silicate wall. The XRD pattern of the functionalized adsorbents also suggests that the structural order of the synthesized material is maintained after functionalization [44].

Nitrogen Adsorption Tests

The nitrogen adsorption-desorption isotherms for mesoporous silicas are shown in Fig. 6. For adsorbent A and adsorbent B, the isotherms are type IV according to the I.U.P.A.C. classification and have an H1 hysteresis loop that is representative of mesopores. The volume of nitrogen adsorbed in the MCM-41 isotherm increased sharply, which represents capillary condensation of nitrogen within the uniform mesopore structure.

Table 1 shows the physical parameters, such the BET surface area (SBET), total pore volume and BJH average pore diameter for mesoporous and amorphous silicas. As expected, the SBET for adsorbent A is higher (546.1 m^2/g) than for adsorbent B (347 m^2/g), whereas the BJH average pore diameter is lower (4.29 nm and 7.90 nm, respectively). In addition, the pore size distribution is narrower in adsorbent A than that in adsorbent B, providing evidence for the uniform framework mesoporosity of the adsorbent A (Fig. 7).

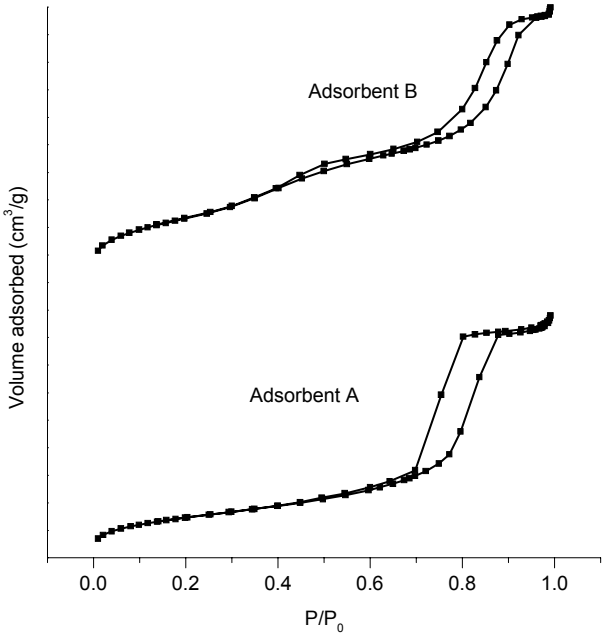

Fig. 6. Nitrogen adsorption–desorption isotherms of adsorbent A and B.

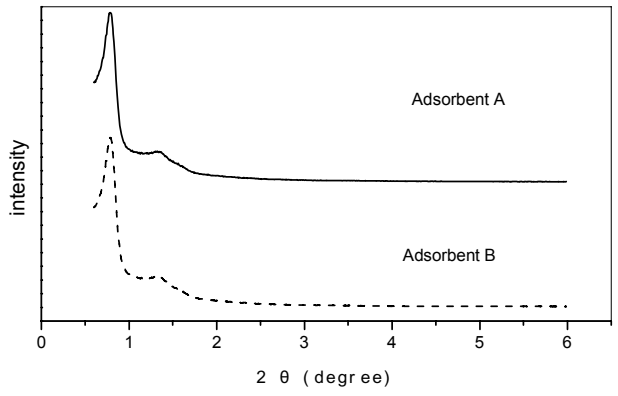

Fig. 5. XRD pattern of adsorbents B and A.

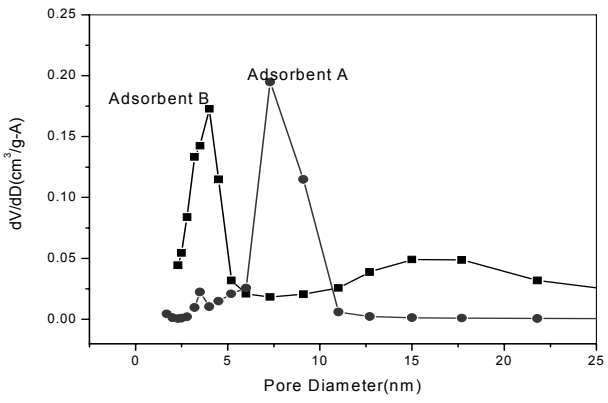

Fig. 7. Pore size distribution of adsorbent A and adsorbent B.

Table 2. Cu^{2+} adsorption on two adsorbents.

Adsorbent	Cu^{2+} (mmol/l)		Removal (%)	Q (mmol/g)	Kd (ml/g)
	C_0	Ce			
A	1	0.011	98.87	0.1977	17,474.54
B	1	0.003	99.68	0.1994	62,300
A	2	0.085	95.77	0.3831	4,529.44
B	2	0.076	96.2	0.3848	5,063.16
A	10	6.256	37.44	0.7488	119.70
B	10	4.759	52.41	1.0482	220.24

Table 3. Zn^{2+} adsorption on two adsorbents.

Adsorbent	Zn^{2+} (mmol/l)		Removal (%)	Q (mmol/g)	Kd (ml/g)
	C_0	Ce			
A	1	0.084	91.61	0.1832	2,184.83
B	1	0.013	98.66	0.1973	14,709.92
A	2	0.108	94.59	0.3784	3,499.01
B	2	0.090	95.51	0.3820	4,250.65
A	10	4.94	50.60	1.0119	204.83
B	10	4.12	58.84	1.1768	285.92

Table 4. Ni^{2+} asorption on two adsorbents.

Adsorbent	Ni^{2+} (mmol/l)		Removal (%)	Q (mmol/g)	Kd (ml/g)
	C_0	Ce			
A	1	0.023	97.73	0.1955	8,612.31
B	1	0.012	98.77	0.1975	16,125.45
A	2	0.151	92.46	0.3698	2,452.96
B	2	0.092	95.42	0.3817	4,168.44
A	10	6.773	32.27	0.6454	95.30
B	10	5.067	49.33	0.9865	194.69

Metal Ion Adsorption on the Functionalized Mesoporous Material

The amount of metal ion on the functionalized mesoporous material can be calculated using the following equations:

$$Q = (C_0 - C_e) \times \frac{V}{W} \qquad (1)$$

$$Kd = \frac{10^3 Q}{C_e} \qquad (2)$$

...where Q is the amount of metal ion on the adsorbents (mmol/g), Kd is the distribution ratio of the metal (ml/g), V is the volume of the aqueous solution (l), W is the weight of the adsorbent (g), C_0 (mmol/L) and C_e (mmol/L) are the initial and equilibrium concentrations of the given ion in solution.

As shown in Tables 2-5, the adsorption capacities were higher for adsorbent B than adsorbent A. Also, these results confirmed that the ureido has a good affect of binding metal ions.

The adsorption ability of different materials such as rice husk was also compared to the mesoporous silica [45-47]. The results were shown in Table 6. It can be seen from the tables that the adsorption of mesoporous materials is better than rice husk, montmorillonite, and bentonite. Because of restrictions of the SBET and pore diameter, the adsorption

Table 5. Co^{2+} asorption on two adsorbents.

Adsorbent	Co^{2+} (mmol/l)		Removal (%)	Q (mmol/g)	Kd (ml/g)
	C_0	Ce			
A	1	0.014	98.65	0.1973	14,607.34
B	1	0.002	99.75	0.1995	79,992.46
A	2	0.151	92.46	0.3698	2,452.96
B	2	0.011	99.47	0.3979	37,761.47
A	10	6.431	35.69	0.7138	110.99
B	10	5.067	49.33	0.9865	194.69

ability is not as good as the industrialized chelated resin. However, as a new functional material, it has an extensive application prospect.

Effect of pH

Since efficiency of the adsorption process is strongly dependent on pH, which affects the existing state of metal ions as well as the surface charge of the ureido functionalization sorbent, experiments on Cu^{2+} were performed. The effect of pH value on Cu^{2+} uptake was studied and the results were shown in Fig. 8. The results clearly show that the removal rate of Cu^{2+} was significantly enhanced from pH 2 to 7, and that the optimum pH for metal removal was 5. The initial concentration of Cu^{2+} was 1 mmol/l.

Metal Ion Competitive Adsorption

The divalent Zn^{2+}, Ni^{2+} and Co^{2+} were selected as adsorptive competing ions with Cu^{2+} because those cations are divalent and have similar ionic radii.

The competitive adsorption of Cu^{2+}, Ni^{2+}, Co^{2+} and Zn^{2+} ions on MCM-41-CTAB and MCM-41-P123 materials are calculated according to Eq. (3) [48]:

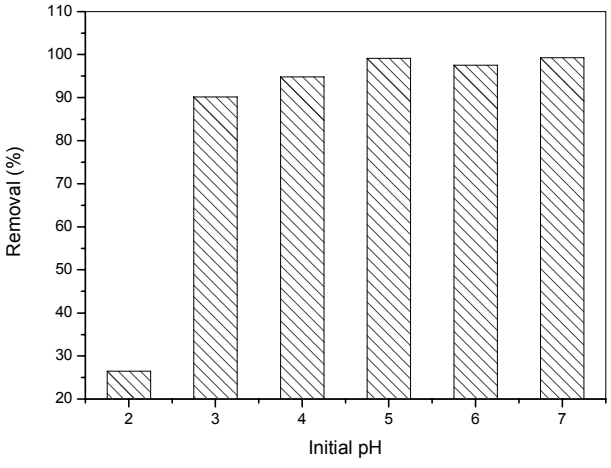

Fig. 8. Removal of Cu (II) as a function of pH (initial Cu(II) concentration is 1 mmol/l, temperature 25ºC).

$$ki = \frac{KdCu^{2+}}{Kdx} \quad (3)$$

...where *ki* represents the ratio of the value of *Kd* of Cu^{2+} to *Kd* of x (Cd^{2+}, Ni^{2+}, Co^{2+}) in mixed solutions. Table 6 summarizes the values for the distribution constants (*Kd*) and selectivity coefficients *ki* of MCM-41 bearing ureido toward Cu^{2+} in the presence of other metal ions.

It was observed that all the ki values were greater than 1, and the Cu^{2+} removal efficiency was still over 90%, though the Cu(II) adsorption amount showed a decrease in the presence of adsorptive competing ions (compared with data in Tables 2-5). This suggests that the adsorptive competing ions in the aqueous solution had little effect on the adsorption of Cu(II) on the adsorbent.

Adsorption Kinetics of Cu^{2+} by Adsorbent B

The Cu^{2+} adsorption kinetic for adsorbent A and adsorbent B exhibits typical pseudo-first-order behavior [41]:

$$q_t = q_{eq}(1 - \exp^{-k_1 t}) \quad (4)$$

...where *t* is the contact time (min); q_t (mmol/g) is the solid-phase loading of metal ions at time *t*; K_1 (min^{-1}) is the rate

Table 6. Comparative of adsorption ability for Cu^{2+} with different materials.

Materials	Heavy metals	Q (mg/g)
rice husk	Cu^{2+}	31.85
	Cd^{2+}	33.2
montmorillonite	Cu^{2+}	32.3
	Pb^{2+}	34.0
bentonite	Cu^{2+}	14.104
	Cd^{2+}	97.8
bentonite	Cu^{2+}	60.2
	Pb^{2+}	368.5

Table 7. Competitive adsorption on the functionalized mesoporous silica of Cu(II).

Solution	Co (mmol/l)	Removal (%)	Kd (mL/g)	ki
$Cu^{2+} + Ni^{2+}$	1	92.40	2,431.58	1.7527
$Cu^{2+} + Co^{2+}$	1	94.32	3,321.13	1.9645
$Cu^{2+} + Zn^{2+}$	1	93.21	2,745.51	2.2329
$Cu^{2+} + Ni^{2+} + Co^{2+} + Cd^{2+}$	1	91.48	2,147.42	1.4169

constants of pseudo-first-order adsorption; q_{eq} (mmol/g) is the adsorption capacity at equilibrium.

Fig. 9 shows the adsorption kinetic of Cu^{2+} ions on adsorbent B by using pseudo-first-order kinetic model. During the initial 3 min., the removal efficiency of Cu^{2+} increased to 99.2%, which clearly illuminated that the extraction process of adsorbent was speeded up in a large scale.

Conclusions

In this work, modified mesoporous silicas (MCM-41) with ureido group were prepared by one-spot procedure using different templates P123 and CTAB. These two adsorbents for binding heavy metals (Cu(II), Zn(II), Co(II), Ni(II)) from aqueous solutions were compared. The results indicate that ureido-Si MCM-41 synthesized by CTAB presents a better potential as an alternative material for heavy metal removal from aqueous solutions than ureido-Si MCM-41 synthesized by P123.

Acknowledgements

The authors gratefully acknowledge the State Key Lab of Pollution Control and Resource Reuse Study of Tongji University, and the water issue project funded by Ministry of Science and Technology (No. 2008ZX07421-002) for the financial support.

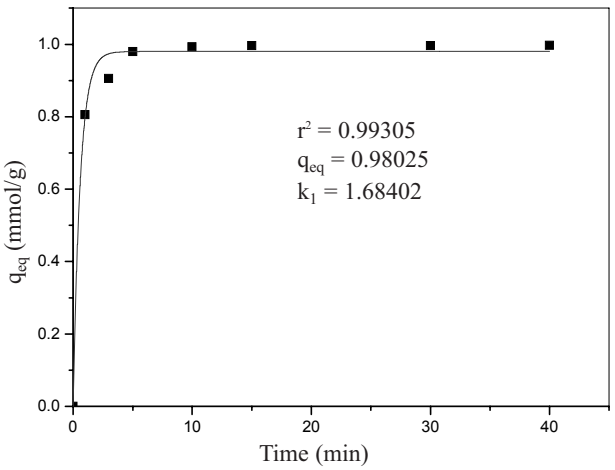

Fig. 9. Pseudo first-order kinetics by nonlinear method for the adsorption of 1 mmol/L Cu(II) solution onto adsorbent B at 298k.

References

1. MERCIER L., PINNANAIA T. A functionalized porous clay heterostructure for heavy metal ion (Hg^{2+}) trapping. Micropor. Mesopor. Mater. **20**, 101, **1998**.
2. BOIS L., BONHOMME A., RIBES A., PARIS B., RAFFIN G., TESSIER F. Functionalized silica for heavy metal ions adsorption. Col. Surf. A: Physicochem. Eng. Aspects. **221**, 221, **2003**.
3. LAGADIC I., MITCHELL M., PAYNE B. Highly Effective Adsorption of Heavy Metal Ions by a Thiol-Functionalized Magnesium Phyllosilicate Clay. Environ. Sci. Technol. **35**, 984, **2001**.
4. CHEREMISINOFF N P. Butterworth., Heineman (Eds.). Handbook of Water and Wastewater Treatment Technologies. **2002**.
5. SINGH D K., SRIVASTAVA M. Selective uptake and recovery of cadmium(II) by microcapsule containing chelating resin. Sep. Purif. Technol. **45**, 1, **2005**.
6. JAL P K., PATEL S., MISHRA B K. Chemical modification of silica surface by immobilization of functional groups for extractive concentration of metal ions. Talanta. **62**, 1005, **2004**.
7. CELIS R., HERMOSIN M C., CONEJO J. Heavy metal adsorption by functionalized clays. Environ. Sci. Technol. **34**, 4593, **2000**.
8. WONG K.K., LEE C.K., LOW K.S., HARON M.J. Removal of Cu and Pb by tartaric acid modified rice husk from aqueous solutions. Chemosphere. **50**, 23, **2003**.
9. WINGENFELDER U., NOWACK B., FURRER G. Adsorption of Pb and Cd by amine-modified zeolite. Water Res. **39**, (14), 3287, **2005**.
10. ÜCER A., UYANIK A., AYGUN S F. Adsorption of Cu(II), Cd(II), Zn(II), Mn(II) and Fe(III) ions by tannic acid immobilised activated carbon. Sep. Purif. Technol. **47**, 113, **2006**.
11. KADIRVELU K., NAMASIVAYAM C. Activated carbon from coconut coirpith as metal adsorbent: adsorption of Cd(II) from aqueous solution. Adv. Environ. Res. **7**, 471, **2003**.
12. DUBOIS G., REYE C., CORRIU R J P., CHUIT C. Organic-inorganic hybrid materials preparation and properties of dibenzo-18-crown-6 ether-bridged polysilsesquioxanes. J. Mater. Chem. **10**, (5), 1091, **2000**.
13. IM H J., YANG Y H., ALLAIN L R., BARNES C.,DAI S.,XUE Z L. Functionalized sol-gels for selective copper(II) separation. Environ. Sci.Technol. **34**, (11), 2209, **2000**.
14. KANG T., PARK Y., CHOI K., LEE J S., YI L. Orderedmesoporous silica (SBA-15) derivatized with imidazole-containing functionalities as a selective adsorbent of preciousmetal ions. J. Mater. Chem. **14**, (6), 1043, **2004**.
15. SAYARI A., HAMOUDI S., YANG Y. Applications of Pore-Expanded Mesoporous Silica. 1. Removal of Heavy Metal Cations and Organic Pollutants from Wastewater. Chem. Mater. **17**, 212, **2005**.

16. KRESGE C T., LEONOWICZ M E., ROTH W J., VARTULI J C., BECK J S. Ordered Mesoporous Molecular Sieves Synthesized by a Liquid-crystal Template Mechanism. Nature. **359**, 710, **1992**.
17. SOLER-ILLIA G J DE A A., SANCHEZ C, LEBEAU B., PATARIN J. Chemical strategies to design textured materials: from microporous and mesoporous oxides to nanonetworks and hierarchical structures.Chem Rev. **102**, 4093, **2002**.
18. LIU Y., PINNAVAIA T J. Aluminosilicate mesostructures with improved acidity and hydrothermal stability.J. Mater. Chem. **12**, 3179, **2002**.
19. STEIN A. Advances in microporous and mesoporous solids highlights of recent progress. Adv. Mater. **15**, 763, **2003**.
20. ZHAO D., HUO Q., FENG J., CHMELKA B F., STUCKY G D. Nonionic triblock and star diblock copolymer and oligomeric surfactant syntheses of highly ordered, hydrothermally stable, mesoporous silica structures. J. Am. Chem. Soc. **120**, 6024, **1998**.
21. ZUKAL A., THOMMES M., CEJKA J. Synthesis of Highly Ordered MCM-41 Silica with Spherical Particles. Micropor. Mesopor. Mater. **104**, 52, **2007**.
22. SAKAMOTO Y., DIAZ I., TERASAKI O., ZHAO D., PARIENTE J P., KIM J M., STUCKY G D., SHIN H J., RYOO R. Direct imaging of the pores and cages of three-dimensional mesoporous material . Nature. **408**, 449, **2000**.
23. SAKAMOTO Y., DIAZ I., TERASAKI O., ZHAO D., PEREZ-PARIENTE J., KIM J M., STUCKY G D. Three-Dimensional Cubic Mesoporous Structures of SBA-12 and Related Materials by Electron Crystallography. J. Phys. Chem. B. **106**, 3118, **2002**.
24. TRONG O D., DESPLANTIERS-GISARD D., DANUMAH C., KALIAGUINE S. Perspectives in catalytic applications of mesostructured materials. Appl. Catal. A. **222**, 299, **2001**.
25. VICEVIC M., BOODHOO K.V. K., SCOTT K. Catalytic isomerisation of α-pinene oxide to campholenic aldehyde using silica-supported zinc triflate catalysts:II.performance of immobilized in a continuous spinning disc reactor.Chem. Eng. J. **133**, 31, **2007**.
26. MELERO J A., CALLEJA G., MARTINEZ F., MOLINA R. Nanocomposite Fe_2O_3/SBA-15: An efficient and stable catalyst for the catalytic wet peroxidation of phenolic aqueous solutions. Chem. Eng. J. **131**, 245, **2007**.
27. P-QUINTANILLA D., HIERRO I DEL., FAJARDO M., SIERRA I. Cr(VI) adsorption on functionalized amorphous and mesoporous silica from aqueous and non-aqueous media. Mater. Res. Bulletin. **42**, 1518, **2007**.
28. SILVA L C C DA., SANTOS L B O DOS., ABATE G., COSENTINOC I C., FANTINIB M C A., MASINE J., MATOS J. Adsorption of Pb^{2+}, Cu^{2+} and Cd^{2+} in FDU-1 silica and FDU-1 silica modified with humic acid. Micropor. Mesopor. Mater. **110**, 250, **2008**.
29. CHOE M J., JANG J Y S. Heavy metal ion adsorption onto polypyrrole-impregnated porous carbon. J. Col. Interf. Sci. **325**, 287, **2008**.
30. WANG H., ZHOU A., PENG F., YU H., YANG J. Mechanism study on adsorption of acidified multiwalled carbon nanotubesto Pb(II). J. Colloid Interface Sci. **316**, 277, **2007**.
31. XUE X M., LI F T. Removal of Cu(II) from aqueous solution by adsorption onto functionalized SBA-16. Micropor. Mesopor. Mater. **116**, 116, **2008**.
32. MURESEANU M., REISS A., STEFANESCU I. Modified SBA-15 mesoporous silica for heavy metal ions remediation. Chemosphere. **73**, 1499, **2008**.
33. HOFFMANN F., CORNELIUS M., MORELL J. Silica-Based Mesoporous Organic-Inorganic Hybrid Materials. Chem. Int. Ed. **45**, 3216, **2006**.
34. STEIN A., MELDE B J., SCHRODEN R C. Hybrid Inorganic-Organic Mesoporous Silicates - Nanoscopic Reactors Coming of Age. Adv. Mater. **12**, 1403, **2000**.
35. LIU A.M., HIDAJAT S., ZHAO D.Y. A new class of hybrid mesoporous materials with functionalized organic monolayers for selective adsorption of heavy metal ions. Chem. Commun. **230**, 1145, **2000**.
36. PEREZ-QUINTANILLLA D., HIERRO I DEl., FAJARDO M., SIERRA I. Mesoporous silica functionalized with 2-mercaptopyridine: synthesis, characterization and employment for Hg (II) adsorption. Micropor. Mesopor. Mater. **89**, 58, **2006**.
37. LIU D., LEI J H., GUO L P., DU X D., ZENG K. Ordered thiol-functionalized mesoporous silica with macrostructure by true liquid crystal templating route. Micropor. Mesopor. Mater. **117**, 67, **2008**.
38. AGUADO J., ARSUAGA J. M., ARENCIBIA A., LINDO M., GASCON V. Aqueous heavy metals removal by adsorption on amine-functionalized mesoporous silica. J. Hazard. Mater. **163**, (1), 213, **2009**.
39. ALGARRA M., JIMENEZ M V., RODRIGUEZ-CASTELLON E., JIMENEZ-LOPEZ A., JIMENEZ-JIMENEZ J. Heavy metals removal from electroplating wastewater by aminopropyl-Si MCM-41.Chemosphere. **59**, 779, **2005**.
40. SAYARI A. Unprecedented expansion of the pore size and volume of periodic mesoporous silica. Angew. Chem. Int. Ed. **39**, (16), 2920, **2000**.
41. YANG H., XU R., XUE X M., LI G T. Hybrid surfactant-templated mesoporous silica formed in ethanol and its application for heavy metal removal. J. Hazard. Mater. **152**, 690, **2008**.
42. PAVIA D., LAMPMAN G., KRIZ G. Introduction to Spectroscopy, Harcourt College Publishers, USA. **2001**.
43. BOIS L., BONHOMME A., RIBES A. Functioalized silica for heavy metal ions adsorption. Colloids Surf. A Physicochem. Eng. Aspects. **221**, 221, **2003**.
44. PEREZ-QUINTANILLA D., SANCHEZ A., HIERRO I del., FAJARDO M., SIERRA I. Preparation, characterization, and Zn^{2+} adsorption behavior of chemically modified MCM-41 with 5-mercapto-1-methyltetrazole. J. Colloids Interf Sci. **313**, 551, **2007**.
45. WONG K. K., LEE C.K., LOW K.S., HARON M.J. Removal of Cu and Pb from electroplating wastewater using tartaric acid modified rice husk. Proce. Biochem. **39**, (4), 437, **2003**.
46. BHATTACHARYYA K G. S. Adsorptive accumulation of Cd(II), Co(II), Cu(II), Pb(II) and Ni(II) from water on montmorillonite: Influence of acid activation. J. Colloids Interf Sci. **310**, (2), 411, **2007**.
47. KUBILAY S., GURKAN R., SAVRAN A., SAHAN T. Removal of Cu(II), Zn(II) and Co(II) ions from aqueous solutions by adsorption onto natural bentonite. Adsorp-J. Inter. Adsorp. Socie. **13,** (1), 41, **2007**.
48. QUINTANILLA D.P., HIERRO I., FAJARDO M., SIERRA I. Adsorption of cadmium(II) from aqueous media onto a mesoporous silica chemically modified with 2-mercaptopyrimidine and chemically modified with 2-mercaptopyrimidine. J. Mater. Chem. **16**, 1757, **2006**.